

UNCLASSIFIED

Defense Technical Information Center  
Compilation Part Notice

ADP012238

TITLE: Surfactant Templated Assembly of Hexagonal Mesostructured Semiconductors Based on  $[\text{Ge}_4\text{Q}_{10}]^{4-}$   $[\text{Q}=\text{S}, \text{Se}]$  and  $\text{Pd}^{2+}$  and  $\text{Pt}^{2+}$  Ions

DISTRIBUTION: Approved for public release, distribution unlimited

This paper is part of the following report:

TITLE: Nanophase and Nanocomposite Materials IV held in Boston, Massachusetts on November 26-29, 2001

To order the complete compilation report, use: ADA401575

The component part is provided here to allow users access to individually authored sections of proceedings, annals, symposia, etc. However, the component should be considered within the context of the overall compilation report and not as a stand-alone technical report.

The following component part numbers comprise the compilation report:

ADP012174 thru ADP012259

UNCLASSIFIED

## Surfactant Templated Assembly of Hexagonal Mesostructured Semiconductors Based on $[\text{Ge}_4\text{Q}_{10}]^{4-}$ ( $\text{Q}=\text{S}, \text{Se}$ ) and $\text{Pd}^{2+}$ and $\text{Pt}^{2+}$ ions.

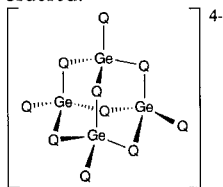
Pantelis N. Trikalitis, Krishnaswamy K. Rangan and Mercouri G. Kanatzidis\*  
*Department of Chemistry, Michigan State University, East Lansing, MI 48824.*

### ABSTRACT

Mesostructured semiconducting non-oxidic materials were prepared by linking  $[\text{Ge}_4\text{Q}_{10}]^{4-}$  ( $\text{Q}=\text{S}, \text{Se}$ ) clusters with the square planar noble metal cations of  $\text{Pd}^{2+}$  and  $\text{Pt}^{2+}$  in the presence of cetylpyridinium surfactant molecules. The use of  $\text{Pt}^{2+}$  afforded materials with exceptionally high hexagonal pore order similar to those of high quality silica MCM-41. These materials are semiconductors with energy band gap in the range  $1.8 < E_g < 2.5$  eV.

### INTRODUCTION

The emergence of the family MCM-X of surfactant templated silica mesoporous molecular sieves with regular pore shape and adjustable pore size a decade ago sparked a flurry of activity worldwide that resulted in an abundance of oxidic mesoporous solids with promising technological properties (1). Whereas these materials will impact catalytic, separation and adsorption applications, they lack interesting electronic properties. Bulk materials that combine mesoscale features and electronic properties are envisioned for novel applications in quantum electronics (2), photonics (3) and non-linear optics (4) among others. Such characteristics may be expected in non-oxidic materials such as the chalcogenides (5). A suitable method for the construction of semiconducting mesostructured materials utilizes a self-assembly process between chalcogenido building blocks and metal cations in the presence of surfactant molecules acting as templates (6). However outstanding issues as to how these systems form remain. The mesostructured chalcogenides reported to date mainly were synthesized by linking adamantane  $[\text{Ge}_4\text{Q}_{10}]^{4-}$  ( $\text{Q}=\text{S}, \text{Se}$ ) clusters (see scheme 1) with first row transition and main-group ions such as Mn, Co, Ni, Zn, Cd, In and Ga, whose coordination preference is mainly tetrahedral. In the exploration of the role of the linkage metal in the assembly process we decided to use noble metal  $\text{Pd}^{2+}$  and  $\text{Pt}^{2+}$  ions because of the strong square-planar coordination preference. Moreover these ions are less kinetically labile than the first-row transition metals and therefore may slow down the self-assembly reaction thus achieving a more ordered structure. In this work we employed the clusters  $[\text{Ge}_4\text{Q}_{10}]^{4-}$  ( $\text{Q}=\text{S}, \text{Se}$ ) with  $\text{Pt}^{2+}$  and  $\text{Pd}^{2+}$  in the presence of cetylpyridinium ( $\text{C}_{16}\text{PyBr}$ ) surfactant molecules. We find that these two similar metal ions behave very differently. In the case of  $\text{Pt}^{2+}$  the materials show remarkable hexagonal pore order similar to those of high quality silica MCM-41 whereas in the case of  $\text{Pd}^{2+}$  the solids are significantly less ordered.



Scheme 1. Chalcogenido adamantane-type  $[\text{Ge}_4\text{Q}_{10}]^{4-}$  ( $\text{Q}=\text{S}, \text{Se}$ ) cluster.

## EXPERIMENTAL

The syntheses of the materials were carried out as follows: 1 mmol of  $\text{TMA}_4[\text{Ge}_4\text{Q}_{10}]$  (TMA=tetramethylammonium; Q=S, Se) was dissolved in 20 ml of formamide at 80 °C. To this clear solution 10 mmol of surfactant  $\text{C}_{16}\text{PyBr}$  was added and the mixture stirred at 80 °C until a clear solution formed. In a flask 1 mmol  $\text{K}_2\text{MCl}_4$  (M=Pt, Pd) was dissolved in 10 ml of formamide and added to the surfactant/ $[\text{Ge}_4\text{Q}_{10}]$  solution dropwise using a pipet. The mixture was aged overnight under stirring and the product was isolated with suction filtration, washed with warm formamide and water and dried under vacuum. The yield was >80 % and the solids were in the form of light powder.

## RESULTS AND DISCUSSION

The mesostructured materials are denoted as  $\text{C}_{16}\text{PyMGeQ}$  where M=Pt, Pd. Unlike in previous cases (6) with other, kinetically labile linkage metals, we observe a considerable slower reaction upon addition of the  $\text{Pt}^{2+}$  metal ions. That is when the  $\text{K}_2\text{PtCl}_4/\text{FM}$  solution was added to the  $\text{C}_{16}\text{Py}/[\text{Ge}_4\text{Q}_{10}]^4$  solution, instantaneous precipitation did not take place. The deposition of the mesophase began 1-1.5 min after and was completed in approximately 10-15 min. As we discuss below the platinum containing mesophases exhibit remarkably good hexagonal mesoscopic order. In contrast  $\text{Pd}^{2+}$  ions, react much more rapidly giving mesophases that exhibit high degree of disorder. Figure 1 shows powder X-ray diffraction patterns of  $\text{C}_{16}\text{PyMGeQ}$  materials. The platinum products show three or four well defined Bragg reflections in the  $2^\circ < 2\theta < 7^\circ$  region, characteristic of mesostructured materials with regular hexagonal pore arrangement. Accordingly these reflections are indexed to a hexagonal  $p6m$  mesophase, see Figure 1. The intense, sharp, well-defined high order reflection (110) and (200) as well as the observation of the fourth (210) reflection, betray a high degree of hexagonal order in these materials as observed directly by transmission electron microscopy (TEM) (see below). In the case of palladium however, the (100) reflection is clearly broader and the high order reflections (110) and (200) are not well resolved, indicating the formation of less ordered mesostructured phases.

Samples of the mesostructured  $\text{C}_{16}\text{PyMGeQ}$  were examined by TEM. Figure 2a shows a characteristic image of  $\text{C}_{16}\text{PyPtGeSe}$  looking down the pore channel axis ([100] direction) where a remarkably uniform hexagonal order is clearly visible. Figure 2b shows a view of  $\text{C}_{16}\text{PyPtGeSe}$  perpendicular to the pore channel axis ([110] direction). The long, straight parallel tunnels are apparent in this image and the observed interpore distances are in good agreement with those obtained from the X-ray diffraction patterns. Similar images were observed in  $\text{C}_{16}\text{PyPtGeS}$  material. Figure 2c,d shows a characteristic image of  $\text{C}_{16}\text{PyPdGeS}$  where the presence of local hexagonal pore arrangement along with disordered regions is evident, as indicated by the X-ray powder patterns. The quality of  $\text{C}_{16}\text{PyPtGeQ}$  solids as judged by the degree of hexagonal order, is comparable to those of high quality silica MCM-41 (7). Figure 3 shows a TEM image of a large  $\text{C}_{16}\text{PyPtGeSe}$  particle where the size of coherent, hexagonally organized domain is >500 nm.

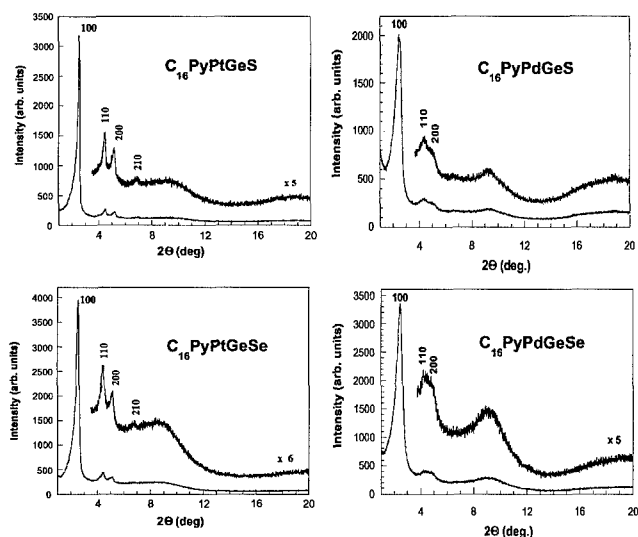


**Figure 1.** Powder X-ray diffraction patterns of mesostructured noble-metal chalcogenides (CuK $\alpha$  radiation).

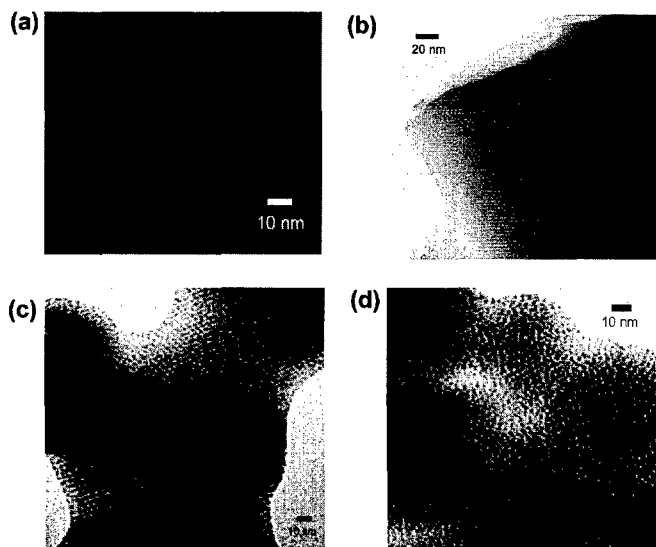


**Figure 2.** Representative TEM images of  $C_{16}PyMGeQ$  materials. (a)  $C_{16}PyPtGeSe$  down to [100] direction, (b)  $C_{16}PyPtGeSe$  down to [110] direction, (c)  $C_{16}PyPdGeS$  down to [100] direction and (d) highly disordered region of  $C_{16}PyPdGeS$ .

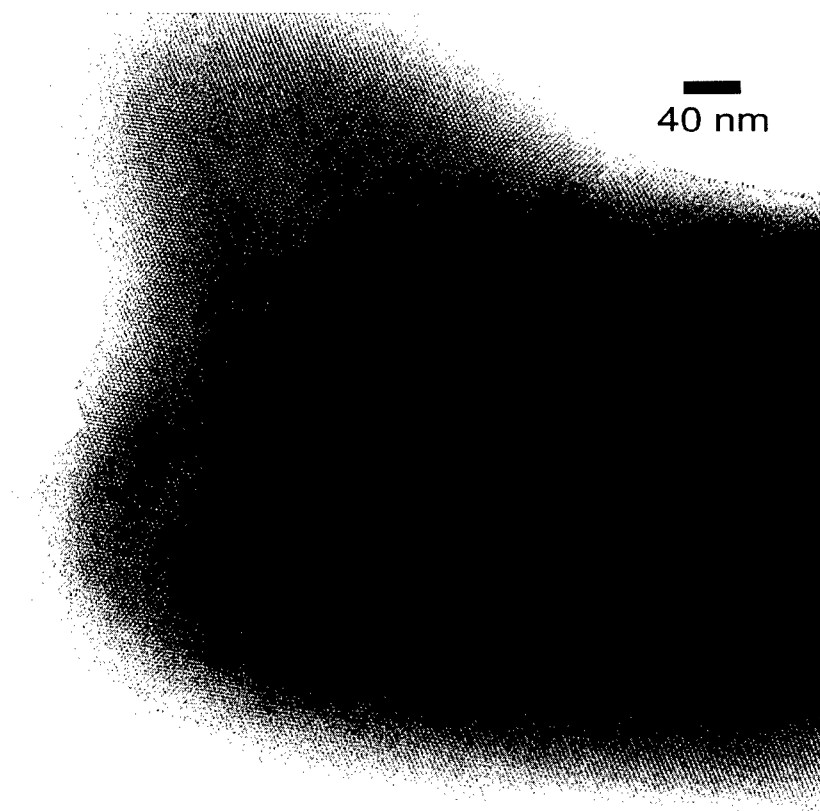
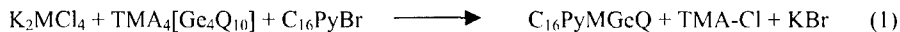


**Figure 3.** Representative image of a large particle of  $C_{16}PyPtGeSe$  showing the hexagonal organization extending over its full body. Particle length  $>500$  nm.

Undoubtedly the quality of the hexagonal pore order in the platinum germanium chalcogenide materials is significantly higher than in palladium analogs. Since the synthesis of  $C_{16}PyPtGeQ$  is based on simple metathesis reactions according to (1),



it is natural to expect that ligand substitution kinetics and coordination preference of the linkage metal ions will affect the quality of the final product. However noble metal ions  $Pd^{2+}$  and  $Pt^{2+}$  exhibit strong square planar coordination geometry. Therefore the striking difference found between  $C_{16}PyPtGeQ$  and  $C_{16}PyPdGeQ$  materials in terms of long range hexagonal pore order, is attributed to the slower reaction observed in the former. In that case, the reactants have more time to react and reach equilibrium thus leading to considerably higher quality hexagonal mesostructured phases.

Infrared (IR) and Raman spectroscopy was used to examine the inorganic framework and also confirm the presence of the surfactant molecules in these materials. In the mid-IR region we observed the characteristic absorption bands of cetylpyridinium cations. Shown in Figure 4a is typical far-IR spectrum from  $C_{16}PyPtGeS$  together with the corresponding spectrum from the free adamantane cluster for comparison. The spectrum of  $C_{16}PyPtGeS$  shows characteristic peaks in the same range as the free adamantane cluster, however, the peaks are much broader indicating possible different bonding environments present.

FT-Raman spectra were collected for the mesostructured  $C_{16}PyPtGeS$  while for the other materials spectra could not be obtained as they decomposed under the laser beam. We observe several vibrational modes attributed to Ge-S and Pt-S stretching modes, see Figure 4b. By comparison with previous Raman studies (6), the sharp peak centered at  $376\text{ cm}^{-1}$  can be assigned to the totally symmetric breathing mode of the " $Ge_4S_6$ " cage, while the peak at  $441\text{ cm}^{-1}$  to terminal Ge-S stretching mode. The peak at  $340\text{ cm}^{-1}$  can be assigned to the Pt-S vibration, according to the spectroscopic analysis of Raman spectrum of PtS.

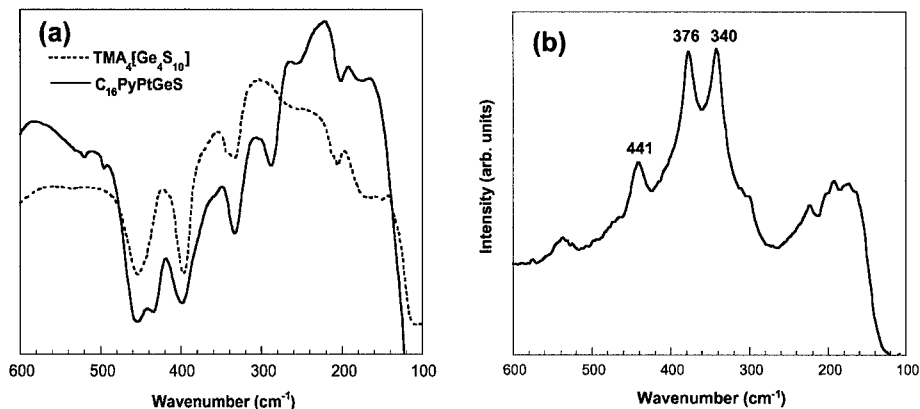


**Figure 4.** (a) Far-IR and (b) FT-Raman spectrum of  $C_{16}PyPtGeS$ .

The optical absorption properties of the  $C_{16}PyMGeQ$  mesostructured materials were investigated with solid state diffuse reflectance UV-vis/Near IR spectroscopy. All solids possess well-defined, sharp optical absorptions associated with bandgap transitions in the energy range  $1.8 < E_g < 2.5\text{ eV}$ , see Figure 5. The bandgap narrows in going from the lighter  $C_{16}PyMGeS$  (Pd:2.5 eV, Pt:2.3 eV) to the heavier  $C_{16}PyMGeSe$  (Pd:2.0 eV, Pt: 1.8 eV). Moreover the effect on the bandgap in going from  $C_{16}PyMGeS$  to  $C_{16}PyMGeSe$  is greater (0.5 eV) rather than in going from  $C_{16}PyPdGeQ$  to  $C_{16}PyPtGeQ$  (0.2 eV) suggesting a more dominant role of the chalcogenide element in the valence and conduction band of the materials.

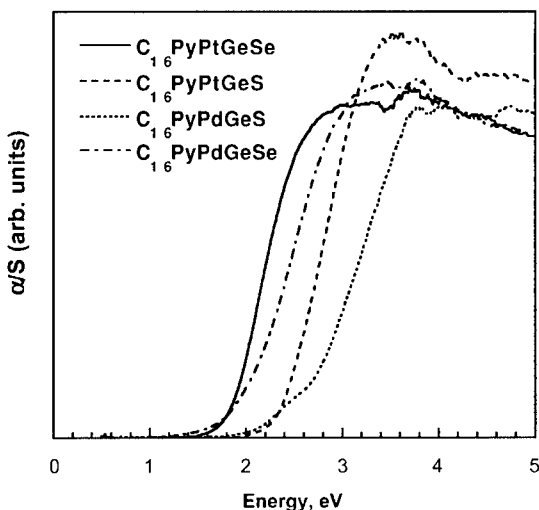


**Figure 5.** Solid state UV-vis absorption spectra of  $C_{16}PyMGeQ$  materials.

## CONCLUSIONS

The use of  $Pd^{2+}$  and  $Pt^{2+}$  as linkage metal ions in a supramolecular assembly of adamantane  $[Ge_4Q_{10}]^{4+}$  clusters leads to a new class of non-oxide mesostructure materials with noble metal ions as part of the framework. In the case of platinum the solids show exceptionally high hexagonal order similar to those in silica MCM-41, whereas in the case of Pd such high order was not observed. This suggests that slower reaction kinetics of framework assembly is an important factor. The materials possess optical bandgaps, ranging between  $1.8 < E_g < 2.5$  eV. The bandgap narrows with the incorporation of heavier elements in the framework.

**ACKNOWLEDGEMENTS** The support of this research by NSF-CRG grant CHE 99-03706 is gratefully acknowledged. This work made use of the SEM and TEM facilities of the Center of Advanced Microscopy at MSU.

## REFERENCES

1. C. T. Kresge, M. E. Leonowicz, W. J. Roth, J. C. Vartuli, J. S. Beck, *Nature* **359**, 710 (1992); Y. Ma, W. Tong, H. Zhou, S. L. Suib, *Microporous Mesoporous Mater.* **37**, 243 (2000); A. Corma, *Chem. Rev.* **97**, 2373 (1997); A. Sayari, P. Liu, *Microporous Mater.* **12**, 149 (1997).
2. P. V. Braun, P. Osenar, S. I. Stupp, *Nature* **380**, 325 (1996).
3. D. J. Norris, Y. A. Vlasov, *Adv. Mater.* **13**, 371 (2001).
4. G. A. Ozin, *Supramol. Chem.* **6**, 125 (1995).
5. H. L. Li, A. Laine, M. O'Keeffe, O. M. Yaghi, *Science* **283**, 1145 (1999).
6. K. K. Rangan, P. N. Trikalitis, M. G. Kanatzidis, *J. Am. Chem. Soc.* **122**, 10230 (2000); K. K. Rangan, P. N. Trikalitis, T. Bakas, M. G. Kanatzidis, *Chem. Commun.*, 809 (2001); P. N. Trikalitis, K. K. Rangan, T. Bakas, M. G. Kanatzidis, *Nature* **410**, 671 (2001); M. J. MacLachlan, N. Coombs, G. A. Ozin, *Nature* **397**, 681 (1999).
7. Q. S. Huo, D. I. Margolese, G. D. Stucky, *Chem. Mater.* **8**, 1147 (1996).